THE LIMBAL PALISADES OF VOGT

BY *William M. Townsend,* MD

INTRODUCTION

THE LIMBAL PALISADES OF VOGT, WHICH WERE DESCRIBED IN THE HUman eye almost a century ago,[1] remain a mystery. The function of this structure, if any, has not been defined, and the anatomy and histology have yet to be fully described. Ultrastructural details have never been published. The purpose of this study is to provide detailed clinical data on this limbal structure, to describe the histologic and ultrastructural features, and to correlate these findings with a possible role in the renewal of the corneal epithelium.

BACKGROUND

The limbal palisades of Vogt were described as "glands" by Henle in 1866 and as "crypts of the conjunctiva" by Dubreuil[2] in 1906, but it was Vogt[3] who, in 1921, presented for the first time a detailed description of the clinical appearance of this structure. Aurell and Kornerup[4] published a light microscopic view of the palisades in 1949. Comparing similar structures in swine, they concluded that the palisades were merely rudimentary accessory lacrimal glands. In 1961, Duke-Elder[5] judged them to be "functionless," thus relegating them to oblivion and obscurity. Ten years later, in a remarkable article published in *Nature,* Davanger and Evensen[6] resurrected them, suggesting a role as a "generative organ for the corneal epithelial cells" but supplying scanty evidence in support of their proposition; Lemp,[7] in his 1976 annual review of the cornea and sclera, also cited the work of Davanger and Evensen. More recently, Goldberg and Bron[8] published an article in the *Transactions* of this Society dealing with biomicroscopic and angiographic aspects of the palisades of Vogt in the normal and abnormal human limbus. The palisades have been mentioned only in passing in some major textbooks on the cornea.[9,10]

There is little doubt that if a function can be ascribed to the palisades of Vogt, it is one related to the renewal of the corneal epithelium in its normal, steady-state condition. The cells of the corneal epithelium and probably those of the entire epibulbar surface exemplify a population

with rapid turnover. Hanna and O'Brien[11,12] described the corneal epithelial renewal rate for various animals and for man: it varies from a short 3 days in some of the former to approximately 10 days in the latter.

Other organs have cell populations with a high turnover rate, including the crypts and villi of the small intestine, the stratified squamous epithelium of the skin, the hematopoietic system, and the seminiferous tubules. Like the corneal epithelium, these tissues have renewal systems that maintain a steady population and avoid exhaustion of the cells. All of these tissues have been studied much more thoroughly than the corneal epithelium, and the findings have demonstrated a number of common features.[13] Each system is composed of three compartments. First, a stem cell[14] compartment provides a reserve pool of self-renewing cells, which are clonogenic and survive for the life of the individual. The stem cells represent a very small fraction of the total population. Morphologically, they appear relatively undifferentiated, with few cytoplasmic organelles or lysosomes. The nuclear chromatin is more evenly dispersed than that of the more differentiated descendants. Nucleoli are large and prominent. Lateral and basal plasma membranes are smooth. Such cells are usually in a reversible noncycling, nonproliferating state designated as G_0. However, an adequate challenge can induce them to proliferate massively. Under steady-state conditions, the two daughter cells resulting from stem cell division show a roughly equal tendency either to remain stem cells or to differentiate further into progenitor cells.[15] Progenitor cells form the second compartment, known as the proliferative or amplifying compartment. This is the actively dividing cell group that serves to replenish the end cell population. Progenitor cells, unlike stem cells, have a limited capacity for cell renewal. They appear committed to the production of daughter end cells.[16] The third compartment is made up of the end cells. These cells have undergone considerable biochemical maturation and have become highly specialized and differentiated. This process usually requires the cells to leave the mitotic cycle permanently in the postmitotic phase (G_1) and, therefore, the end cells lack the capacity to divide.[17]

By analogy, it seems logical to assume that the undisturbed corneal epithelium can also be characterized in terms of these three compartments. Some of the aspects of these compartments have actually been described in various publications, but they have never been identified as such. Hanna and O'Brien[11] observed the uptake of tritiated thymidine by only the two lower layers of the cornea. By definition, the nondividing cell population above those basal cell layers must represent the end-cell compartment, while the basal layers fit in the category of progenitor cells. After a basal cell divides, the two daughter basal cells may divide again as

new progenitor cells, or as is more likely, may differentiate into end cells. This pattern of division is known as symmetric, and appears to be the most common one in all of the other systems.[15] In the intestinal epithelium, most divisions in the lower part of the crypt supply additional progenitor cells. In order to maintain a steady state, an equal number of divisions in the upper part of the proliferative zone must generate end cells. In the corneal epithelium, that zone may be represented by the more superficial of the two basal layers.

In mouse skin, the epidermal end keratinocytes are derived from groups of 10 or 11 basal cells that integrate to form a so-called epidermal proliferative unit (EPU).[18] Each EPU contains one stem cell that occupies a more or less central position within the basal layer of the unit. As progenitor cells in the basal layer begin to divide, they are pushed laterally to the boundaries of the EPU. Continued proliferation eventually shifts those cells into the overlying layer, where they differentiate into end cell keratinocytes.[19] Each basal cell measures only 6 to 10 μm, whereas the daughter cells increase in size as they move toward the surface, reaching as much as 30 to 45 μm. Thus, 100 basal cells occupy the same area as only 20 overlying keratinized cells. For this reason, relatively few mitoses suffice for the replacement of end cells.[20] Furthermore, the vertical transit from basal cell to stratum corneum takes about 2 weeks, and another 2 weeks pass before the end cell is finally sloughed. This relatively slow transit time also helps to account for the low mitotic index of the basal cell in the undisturbed epidermis (0.1 to 1.0 per 1000 cells).[16]

In the corneal epithelium, in contrast, the area occupied by each basal cell is nearly the same as that of the overlying wing cell. Furthermore, the turnover rate in the corneal epithelium greatly exceeds that of the epidermis. In the mouse, Bertalanffy and Lau[21] reported mitotic rates of 14 and 3 for cornea and skin epithelium, respectively. These huge demands emphasize the greater proliferative requirement of the corneal epithelium compared to the epidermis. Yet the ability of the basal cell layer to satisfy such requirements is questionable in view of the fact that it lacks a stromal element. This appears to be an essential component in all other formative systems.[22] Davanger and Evensen[7] suggested that the palisades of Vogt represent true papillae composed of vascularized stroma analogous to those of skin and, therefore, could be the actual stem cell compartment for the corneal epithelium. Supportive data have come from Schermer and associates,[23] who showed that a major differentiation product, 64K keratin, is present uniformly in all the layers of the central corneal epithelium but only suprabasally in the limbal region. They suggested that the evidence pointing to the limbal cell as the more

undifferentiated one implies that the limbal cell layer is the locus of the stem cell population.

Identification of the stem cell has proven much more difficult for epidermis than for the other organ systems previously mentioned. However, in 1982 Lavker and Sun[24] identified two distinct populations of basal keratinocytes: serrated and nonserrated. In the more detailed report that followed,[25] they presented evidence supporting the view that the nonserrated basal cells are the actual stem cells of the epidermis. The serrated basal cells are located in the shallow rete ridges. The nonserrated basal cells occupy the tips of the deep rete ridges. The authors concluded that, in the serrated basal cells, the well-developed cytoplasmic projections extending into the dermis serve an anchoring function. The nonserrated basal cells lack such projections, presenting a much smoother epidermal-dermal interface. They also have a greater nuclear-cytoplasmic volume ratio and appear smaller, and cuboidal rather than columnar in shape. Like the cytoplasm of other, more undifferentiated cells, the cytoplasm of the unserrated basal cells is rich in free ribosomes whereas keratin filaments are scarce.

If the limbus is the locus for the stem cell compartment, then the daughter progenitor cells must have quite a journey in order to cover the basal region of the entire corneal surface. Much information is available suggesting that such transit does occur. Working with the rat and using flat preparations, Buschke and co-workers[26] found an interesting topographic pattern. Mitoses were more numerous in the peripheral than in the central region of the cornea, revealing a meridional gradient directed centripetally. The greater proliferative capacity of the limbal cornea relative to the central region has also been demonstrated by other authors.[27,28] In other organ systems, the proliferative compartment is physically located adjacent to the stem cell compartment. Similarly, the more limbal cornea, by virtue of its greater proliferative capacity, may indicate its proximity to the stem cell compartment. The gradient may also indicate a centripetal transit of progenitor basal cells. Kaye[29] observed the centripetal migration of epithelial microcysts from the periphery of corneal transplants followed over the course of several months. Also in transplants, Kinoshita and associates[30] detected a gradual dilution of donor epithelial cells, identified by their chromatin bodies; the donor cells from the center of the (donor) cornea were slowly replaced by peripheral recipient epithelial cells. Shapiro and colleagues[31] isolated the central epithelium from that of the periphery in rabbits. They were able to document that central to the barrier the epithelium became thinned while the peripheral region thickened, suggesting a centripetal cellular flow.

Several additional publications lend support to the concept of centripetal movement. Buck,[32] working with mice, observed that peripheral cells marked with India ink moved several millimeters toward the central cornea during the healing of abrasions in the latter region. A much slower rate was recorded in the steady state in nonwounded mouse corneas.[33] In 1944, Mann[34] described the central displacement of limbal pigment in the injured corneas of both rabbits and humans. The displaced limbal pigment assumed a radial pattern directed centripetally towards the wound. In 1963, Cowan[35] used the term "striate melanokeratosis" to describe radial, vortex-shaped, striated lines of golden-brown pigment in blacks with chronic epithelial lesions. He distinguished his cases from those described by Mann by noting that the pigment element was largely the result of the presence of melanocytes under the epithelium rather than melanin granules within basal cells.

Bron,[36] in his excellent thesis on the vortex pattern of the corneal epithelium, made additional correlations which further identify the manner of the centripetal movement. He observed the vortex pattern in injured corneas, as had Mann, but, in addition, he linked the pattern with what is seen in numerous epitheliopathies. These conditions, now identified as lysosomal storage diseases, may be of exogenous origin, such as those associated with prolonged use of chloroquine, mepacrine, amodiaquine, amiodarone, indomethacin, chlorpromazine, urethan, and pethidine, or endogenous, such as Fabry's disease. The accumulated deposits that characterize the storage diseases serve to mark the basal cells and thereby reveal the path followed during their centripetal migration, much in the same fashion that melanin marks the basal cells in the cases described by Mann.

In 1983, Thoft and Friend[37] proposed the *X*, *Y*, *Z* hypothesis of epithelial maintenance. *X* denotes the vertical proliferation, *Y* the horizontal or lateral migration, and *Z* the cell loss from the surface. To maintain equilibrium, *X* plus *Y* must equal *Z*. The concept does not take into account conditions that may affect the proliferative and stem cell compartments, but it is useful in bringing into focus how the equilibrium of epithelial renewal may be perturbed. Any condition that inhibits or retards the mitotic process or that alters the epithelial slide or leads to excessive loss from the epithelial surface could lead to such a perturbation. Table I lists conditions that are known to affect the steady state of normal epithelial renewal.

TABLE I: CONDITIONS THAT MAY ALTER EPITHELIAL RENEWAL*

MITOSIS INHIBITION	SLIDING INHIBITION	INCREASED SURFACE LOSS
Epithelial wound[38]	Heat[55]	Ultraviolet radiation[61]
Cooling and freezing[39]	Burn injury[55]	Adenine arabinoside[62]
Local pH changes[39]	Cold[55]	Idoxuridine 0.1%[62]
Chalones[40]	Anoxia[56]	Trifluorothymidine[62]
X-radiation[41]	Cyanide[55]	Soft and hard contact lenses[63]
Beta radiation[42]	Metabolic inhibitors[57]	Benzalkonium chloride[64]
Colchicine[43]	Topical anesthetics[58]	Phospholine iodide[64]
Immunosuppressors[44]	Topical steroids[59]	2% pilocarpine[64]
Topical anesthetics[45]	Fibronectin deficiency[60]	Phospholine iodide[64]
Denervation[46]		4% cocaine[64]
Catecholamines[47]		Neomycin[64]
Cyclic AMP[48]		Loss of lacrimal gland[65]
Unwashed lanolin[49]		Exposure[66]
Fright or fight[50]		Keratitis sicca[67]
Circadian rhythm trough[51]		Hypertonicity of tear film[68]
Avitaminosis A[52]		Neuroparalytic keratitis[69]
Malnutrition[53]		Chemical burns[70]
Hypophysectomy[54]		Keratoplasty[71]

*Many determined only in animals under experimental conditions.

MATERIALS AND METHODS

CLINICAL OBSERVATIONS

Biomicroscopic Evaluation of Normal Pattern and Variations

Individuals with normal anterior segments were examined with the Zeiss slit lamp model 30 SL/M. Subjects were consecutively placed into one of six groups until the full complement of 50 was reached in each group. The six groups were characterized as follows: less than 40 years old or over 40; male or female; lightly pigmented or heavily pigmented subject. The observed palisade pattern was recorded in each subject and measured with a micrometer graduated in 0.01-mm steps. Representative subjects were photographed using a 50/50 beam splitter, 2× magnification tube, and Contax camera with 3M 640 T film.

Illustrative Case Reports

Twenty-two patients suffering from chronic epithelial disturbances were observed to show the vortex pattern over a period of 3 years. Brief case reports and fluorescein patterns of five illustrative cases are presented.

HISTOLOGIC STUDIES

Flat Preparations

Forty-six isolated human corneas were obtained from the Lions Eye Bank. The donor corneas had been declared unsuitable for transplantation because the donor had a positive enzyme-linked immunosorbent assay (ELISA) for human immunodeficiency virus (HIV), a positive reading for hepatitis B virus, or because the blood obtained for testing was hemolysed, thereby making such tests impossible to carry out. The corneas were transferred from McCarey-Kaufman (M-K) or K-Sol medium to 10% buffered formalin no later than 48 hours postmortem. The central region was removed from each cornea, leaving a 5-mm rim composed of peripheral cornea, limbus, and scleral border. The rim was then divided into four segments labeled superior, inferior, nasal, and temporal. Each segment was further bisected; one half served for flat preparations while the remainder was destined for serial sectioning.

Each specimen intended for flat preparation was thinned to about one third corneal thickness using a No. 15 Bard-Parker blade. The specimen was transferred to 70% ethyl alcohol and, after 12 hours, stained with a modified Harris hematoxylin and eosin method. After hydration in 60% and 50% ethyl alcohol and tap water (10 minutes each), the specimen was placed in freshly prepared hematoxylin for a period of 4 minutes. After differentiation for 30 seconds in acid alcohol and then blueing for 60 seconds in a saturated lithium carbonate solution, the specimen was washed in tap water for 10 minutes and stained with acid eosin for 30 seconds. Following dehydration in two changes of 95% and absolute alcohol, each specimen was cleared in xylene and mounted in Permount (Fisher).

Serial Sections

The segment intended for serial section was processed routinely and stained with standard stains,[72] including Harris' hematoxylin and eosin, periodic acid-Schiff, and Masson. Most of the sectioning was oriented in the coronal plane, although a few specimens were cut radially in order to obtain a longitudinal view of the palisades.

ULTRASTRUCTURE

Human corneas that had been placed in M-K medium within 6 hours postmortem and later declared unfit for transplantation were obtained from the eye bank. Within 48 hours postmortem, the corneas were fixed in 2.5% glutaraldehyde. The limbal region was isolated and divided into

1-mm squares under the dissecting microscope. The specimens were postfixed in 1% osmium tetroxide at 4°C, dehydrated in a series of graded alcohols, and infiltrated with a plastic embedding medium. Sections 1 μm thick were cut from selected blocks on the ultramicrotome and stained with 1% toluidine blue. Thin sections were cut from appropriate blocks, triple-stained with lead acetate, uranyl acetate, and Reynold's lead citrate, and processed for electron microscopic examination.

RESULTS

CLINICAL OBSERVATIONS

Biomicroscopic Evaluation

The palisades of Vogt appeared as parallel rows of fine longitudinal ridges or cords located in the limbus and disposed radially around the corneal surface (Fig 1A). The ridges, to quote Duke-Elder,[5] resembled "ribs of sand in the seashore," particularly when viewed by sclerotic scatter illumination. Each ridge could be distinguished from the adjacent conjunctiva by its more intense white color and its sharply defined borders (Fig 1B). In heavily pigmented individuals the edges of the palisades were often outlined by a rim of brown pigment that rendered the structure more easily visible (Fig 2A). In some palisades the pigment rim continued without interruption to close off either the corneal or conjunctival end. The shape of the individual ridges frequently varied within the same palisades complex. Sometimes the ridges appeared to branch into Y- or V-shapes; on occasion they interconnected, producing a trabeculated pattern (Fig 2B). In some cases, ridges were seen to break off abruptly in association with a minuscule oval just beyond the termination.

The dimensions of the palisades at the inferior limbus measured in 200 normal subjects (Table II) revealed considerable variation in the length of the structure as well as in the number of units present per subject, even when the same region was used for measurement. The mean number of ridges was 36 (range, 1 to 64). The length of the ridges varied from 0.09 mm to 0.86 mm (mean, 0.31 mm). The width of the palisades and the distance between palisades in the two eyes of a single individual was symmetric, with much similarity in comparable limbal regions.

The configuration of the palisades in the population studied showed one of three major patterns. In the standard pattern (Fig 1A), the palisades are thin cylindrical ridges, 0.31 mm long and 0.04 mm wide, fairly evenly spaced, with little or no pigmentation. The exaggerated pattern (Fig 2A) was characterized by palisades of considerably greater width, greater degrees of pigmentation, and a tendency toward trabeculation, as well as variability in shape; streaks of golden-brown pigment were often

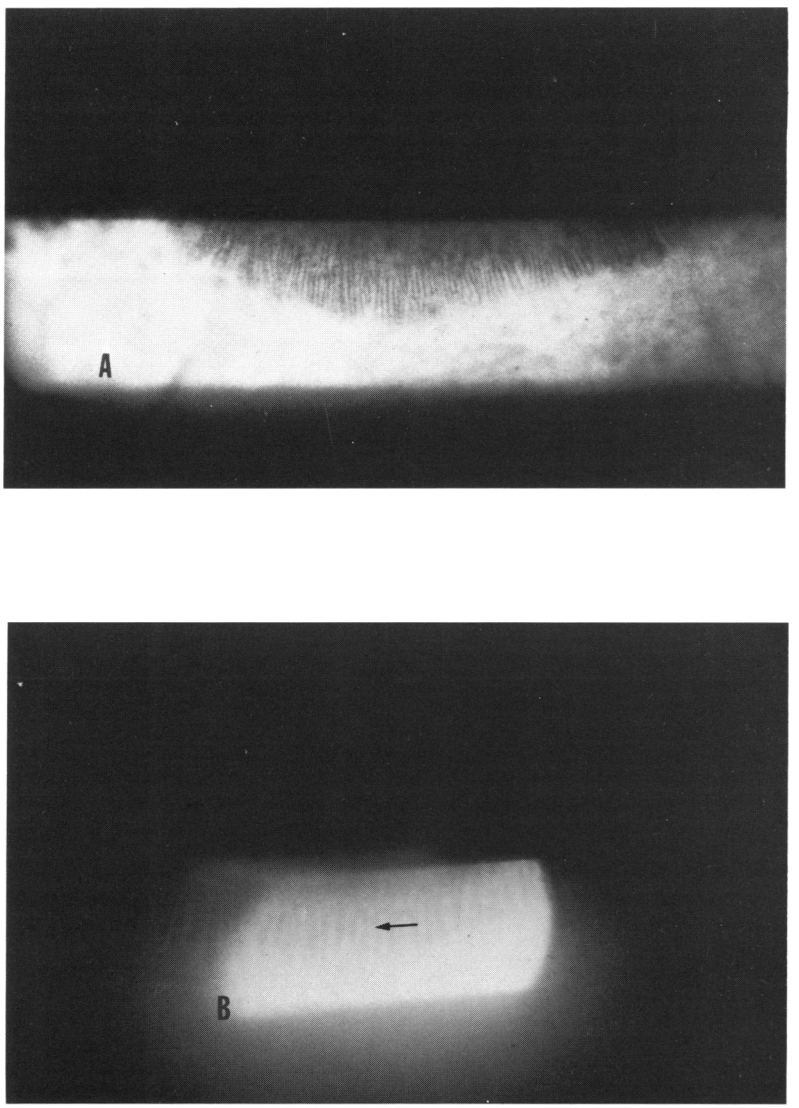

FIGURE A: Standard configuration of palisades of lower limbus. Mildly pigmented borders outline rim of individual ridges. B: Attenuated palisade pattern. Inferior limbus of 28-year-old white female. *Arrow* points to whitish appearance of ridges when illuminated indirectly.

TABLE II: PALISADE DIMENSIONS IN 200 NORMAL SUBJECTS*

	NO.	LENTH	WIDTH	SEPARATION
Mean (mm)	36	0.31	0.04	0.09
Range (mm)	1-64	0.09-0.96	0.03-0.06	0.06-0.12
SD (mm)	± 2	± 0.08	± 0.01	± 0.02
Coefficient of variation (%)	—	46.3	20.1	24.5

*In inferior limbus.

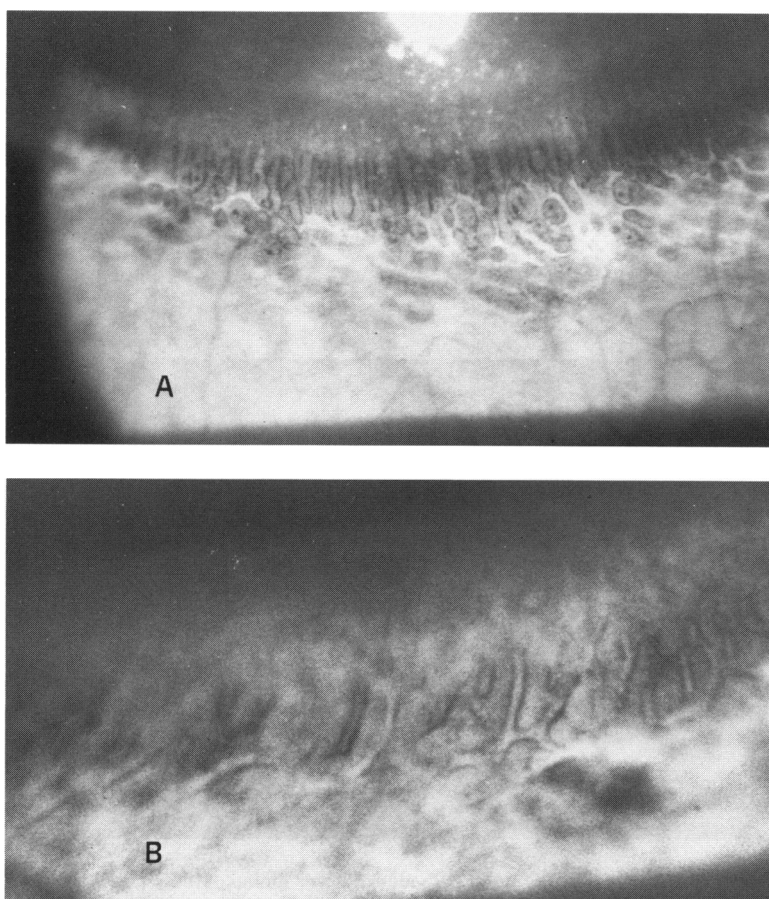

FIGURE 2

A: Exaggerated pattern of palisade configuration in lower limbus of 61-year-old highly pigmented male. Individual ridges appear broader than in standard type of palisades. B: High-power view of exaggerated pattern in lower limbus of 57-year-old highly pigmented male. Branching ridges join to produce trabeculation.

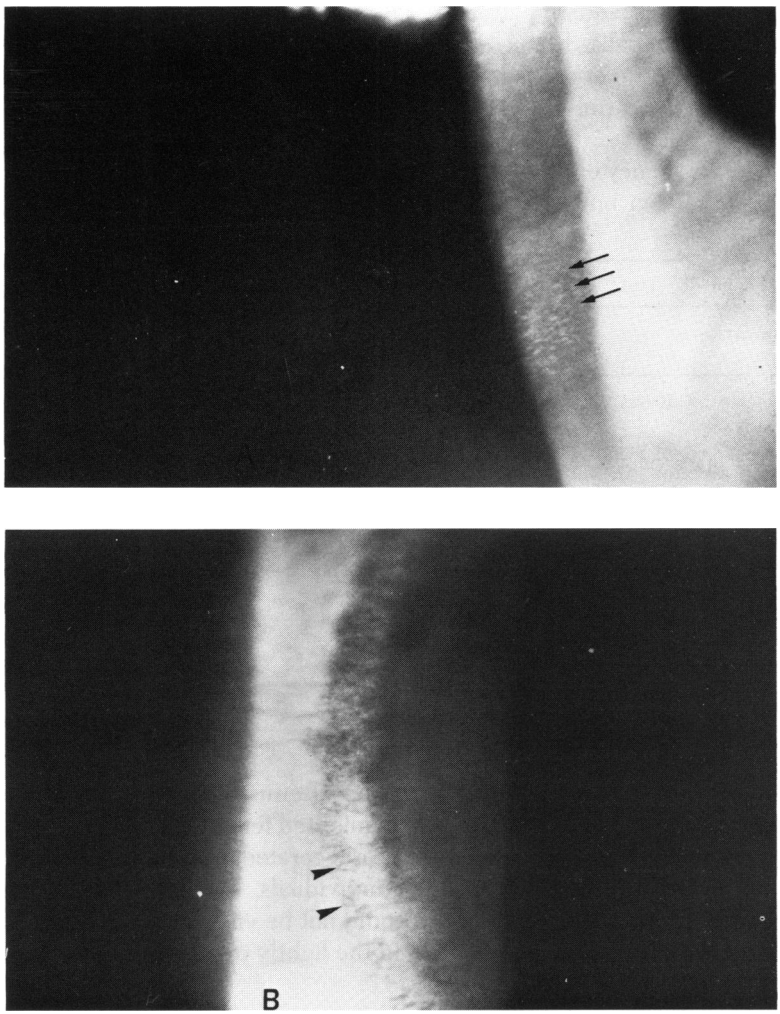

FIGURE 3
A: Highly magnified slit lamp view of epithelial surface in a normal 48-year-old Nego. *Arrow* points to linear streaks that extend radially from limbus into cornea. B: Palisade pattern along horizontal limbal region in highly pigmented 37-year-old male. Minute palisade oval ridges indicated by *arrows*.

seen within the cornea pointed radially toward the center (Fig 3A). In the attenuated pattern (Fig 1B), the palisade ridges were thinner and more delicate than in the standard pattern.

In a given subject, the two limbal zones usually demonstrate different

patterns. The standard pattern was most frequently present in the inferior limbus. The palisades in the superior limbus were usually attenuated relative to those of the inferior limbus. The horizontal quadrants (Fig 3B) usually showed only miniature ovals, small size "fragments," or none at all.

The frequency of the patterns was assessed in the six groups composing the population under study (Table III). The prevalence of the standard

TABLE III: PALISADE CONFIGURATION IN 200 NORMAL SUBJECTS*

	STANDARD		EXAGGERATED		ATTENUATED		UNDETECTED	
	NO.	%	NO.	%	NO.	%	NO.	%
Group A (< 40 yrs) $n = 50$	15	30	5	10	25	50	5	10
Group B (> 40 yrs) $n = 50$	15	30	5	10	20	40	10	20
Males $n = 50$	15	30	5	10	25	50	5	10
Females $n = 45$	10	22	5	11	25	56	5	11
Light P $n = 50$	13	25	0	0	27	55	10	20
Heavy P $n = 46$	15	33	6	13	19	41	6	13

*In inferior limbus.
P, individual pigmentation.

pattern was similar in all groups. The attenuated pattern, which was observed most commonly in lightly pigmented females, showed the greatest prevalence in each group. The exaggerated pattern was most frequently seen in heavily pigmented individuals, but not at all in lightly pigmented subjects. The palisades could not be visualized at all in 10% to 20% of the population, particularly in the lightly pigmented and the older age group.

CASE REPORTS

CASE 1

A 64-year-old white male was referred in consultation. The patient had been treated for 8 years for Sjögren's syndrome. Symptoms and findings caused by the dry eye condition had been stable until 3 weeks previously, when severe epithelial defects appeared in both corneas. Despite the increased use of artificial tears without preservatives as well as the application of bandage soft lenses and then occlusive bandages, no improvement was recorded. The patient had been taking oral azathioprine for the previous 6 weeks to treat severe arthritis. Bilateral

extensive corneal abrasions were present on examination. Fluorescein application revealed the presence of linear staining in the form of numerous, confluent streaks that arose from the edges of the defect and radiated toward the limbus (Fig 4). The lesions subsided after azathioprine was discontinued but reappeared when the medication was later prescribed by a physician who was unaware of the patient's previous history.

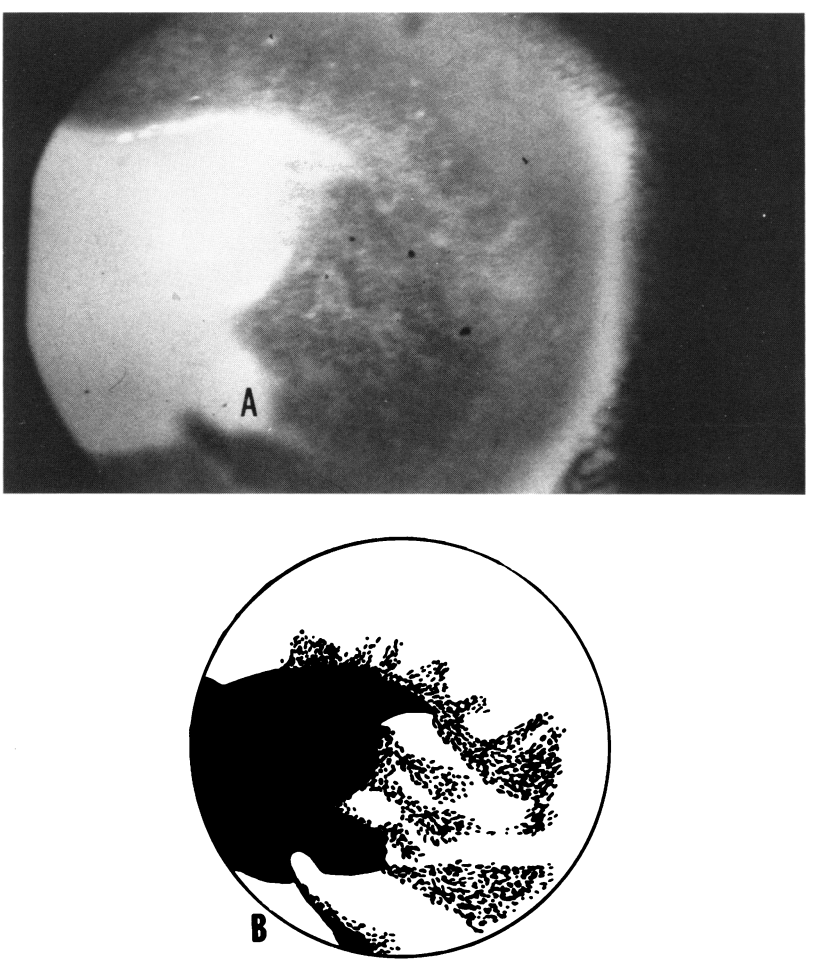

FIGURE 4
A: Fluorescein pattern in a 64-year-old male with Sjögren's syndrome. B: Drawing of pattern of fluorescein staining observed in A. Staining reveals radially oriented linear streaks that broaden toward limbus.

CASE 2

A 52-year-old female teacher with subclinical lacrimal deficiency was referred in consultation when severe symptoms appeared in the left eye. One week previously, a "dermolipoma" had been excised from that eye. Pathologic examination of the tissue showed that the specimen included most of the lacrimal gland. The left cornea showed confluent streaks of fluorescein staining that assumed a spoke-wheel or vortex pattern. The spokes were directed radially toward the limbus with the axis near the center of the cornea (Fig 5).

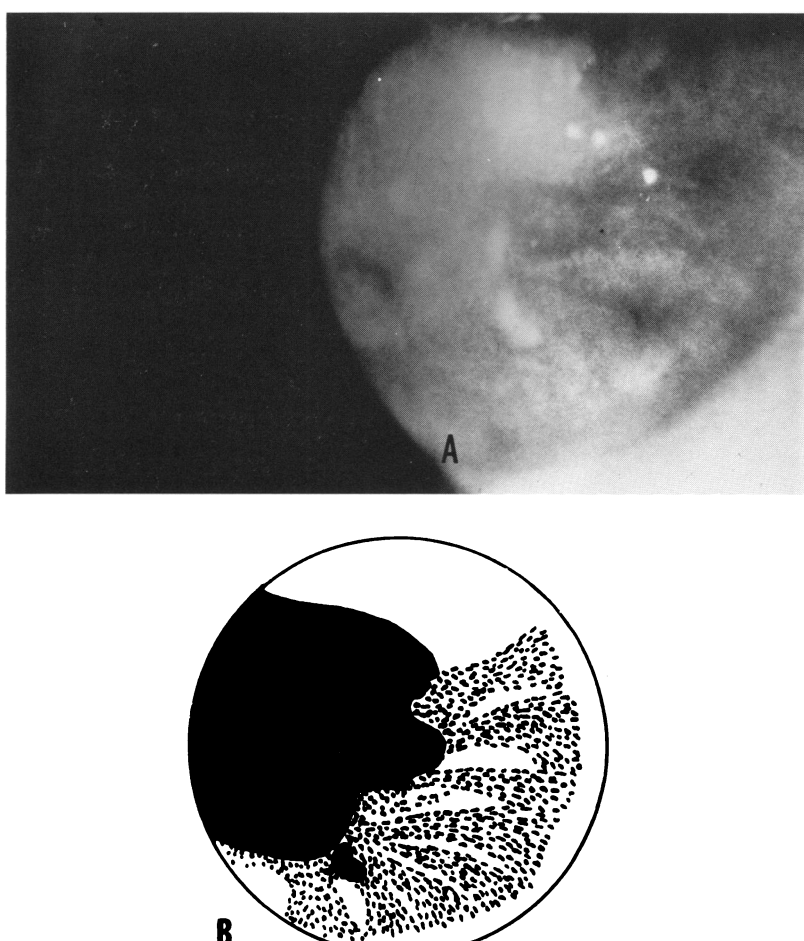

FIGURE 5

A: Fluorescein pattern in a 52-year-old female who developed severe lacrimal deficiency after lacrimal gland was mistakenly excised from left eye. B: Drawing of fluorescein pattern observed in A. Beyond the central edematous bare stroma, a spoke-wheel pattern is formed by confluent linear staining streaks that broaden toward limbus.

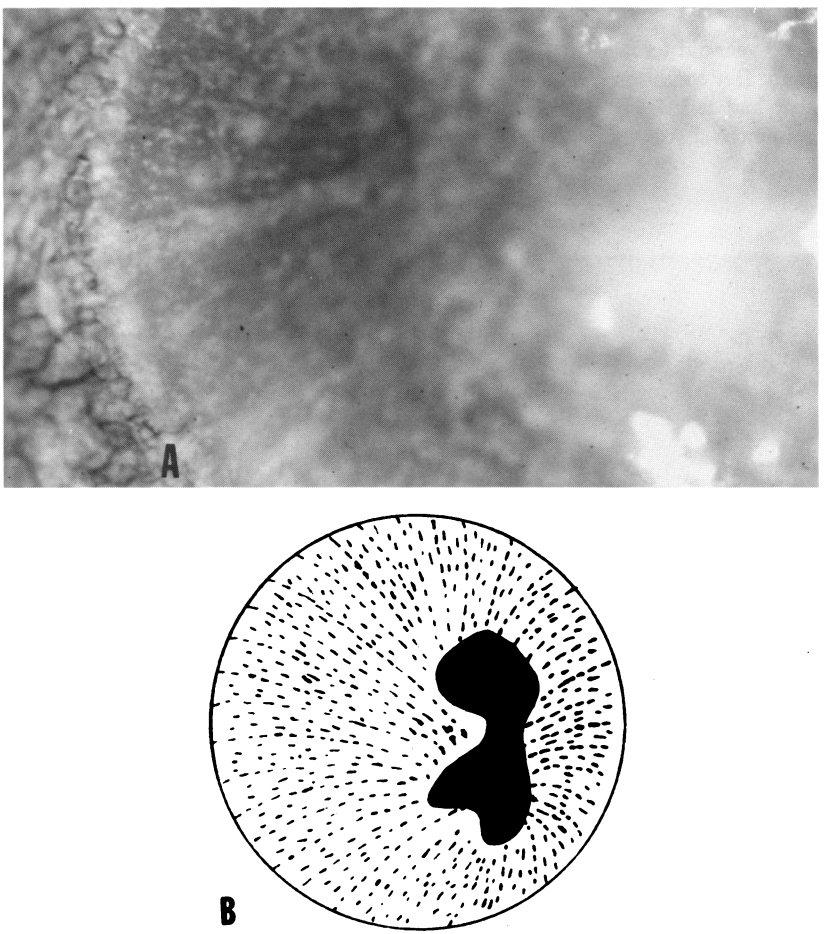

FIGURE 6
A: Fluorescein pattern in a 46-year-old male with chronic herpetic ulceration of right eye. B: Drawing of fluorescein pattern observed in A. Linear streaks of fluorescein staining extend toward limbus from margins of ulcer.

CASE 3

A 46-year-old male was referred in consultation when a herpetic central corneal ulcer persisted despite 2 months of treatment with antiviral agents. The right eye showed a central, rectangular epithelial defect with sharp borders and little infiltration. Fluorescein application disclosed the presence of streak-staining that formed a spoke-wheel or vortex pattern directed radially toward the limbus from the borders of the defect (Fig 6).

CASE 4

A 68-year-old female was referred in consultation with the diagnosis of keratitis sicca. Her condition worsened with the development of bilateral epithelial defects that had failed to heal in 2 months. Examination disclosed the presence of conjunctival scarring with early symblepharon formation, indicative of cicatricial

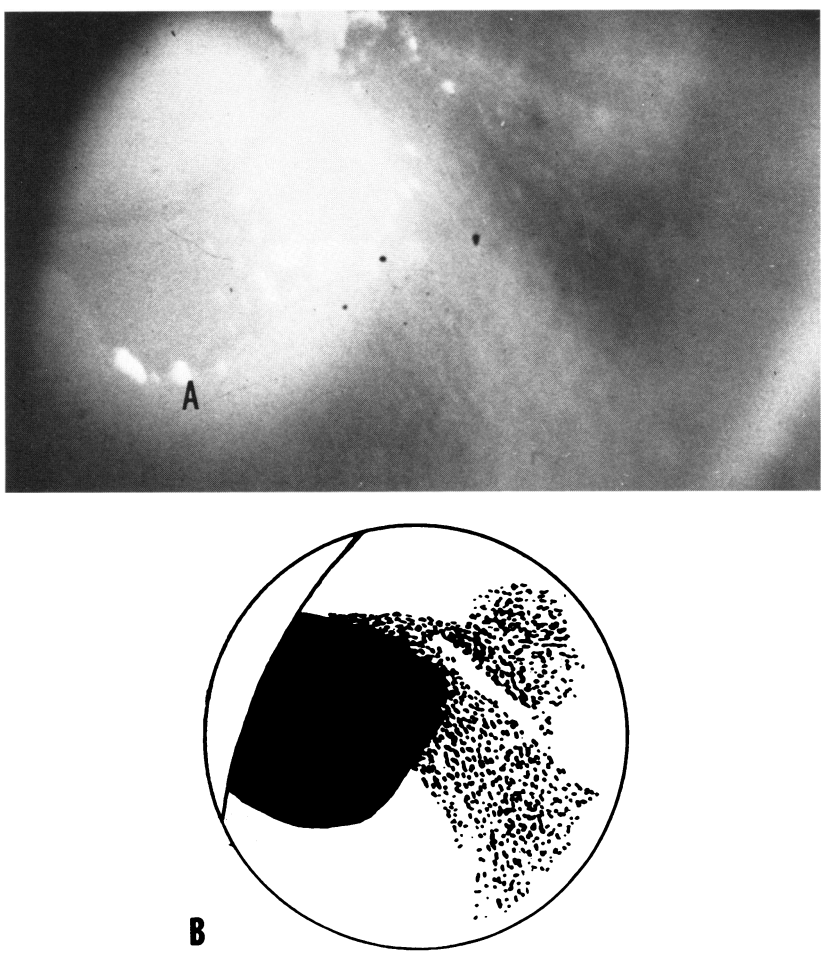

FIGURE 7

A: Fluorescein pattern of left cornea in a 68-year-old female with bilateral chronic epithelial defects caused by senile cicatricial pemphigoid. B: Drawing of fluorescein pattern observed in A. Linear streaks of fluorescein staining extend toward limbus from edge of ulceration.

senile pemphigoid. Both corneas showed central oval defects without stromal infiltration or vascularization. The application of fluorescein revealed the presence of linear streak-staining that assumed a spoke-wheel or vortex pattern directed toward the limbus (Fig 7).

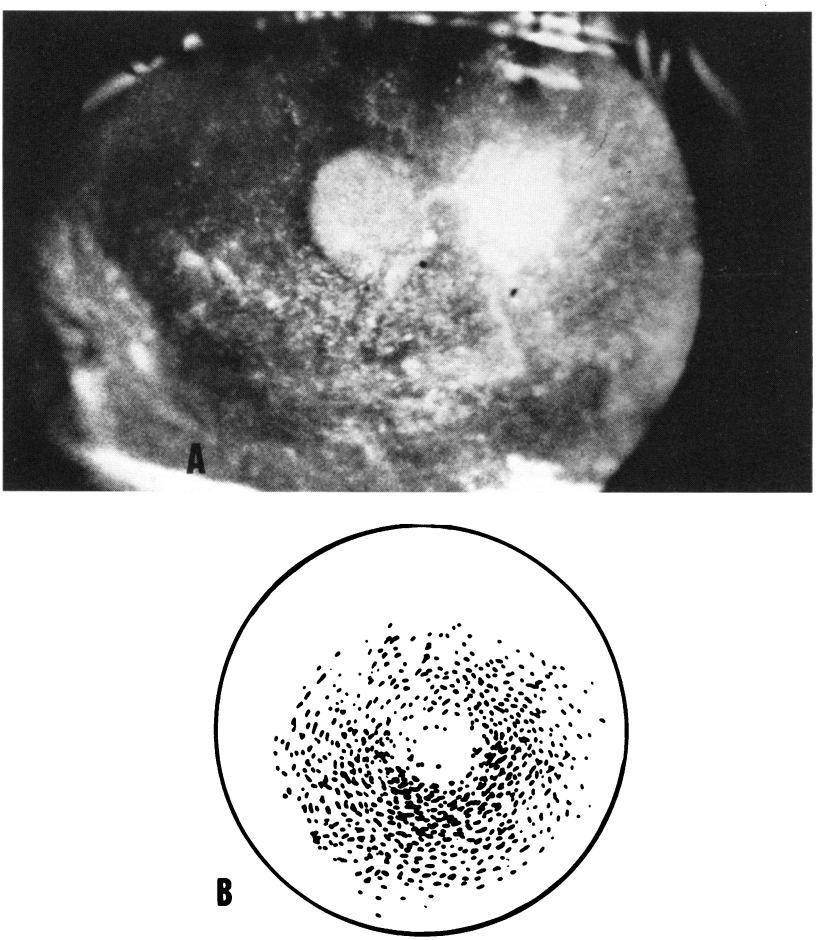

FIGURE 8

A: Fluorescein pattern of right cornea in a 75-year-old male whose epithelium had been undisturbed during the first 6 weeks after keratoplasty. B: Drawing of fluorescein pattern seen in A. Streak-staining within graft center displays a vortex configuration.

CASE 5

A 75-year-old male underwent partial penetrating keratoplasty of the right eye for aphakic bullous keratopathy. The donor cornea was obtained from a 22-year-old male. The tissue was placed in M-K medium less than 8 hours postmortem and was used for grafting within 48 hours. No epithelial disturbance was noted at surgery or during the first 6 weeks postoperatively although the tear meniscus in both eyes was almost absent and the Schirmer II test produced zero readings. Medications included artificial tears four times a day and timolol 0.5% twice a day. The patient presented with streak-staining of the graft epithelium in a vortex configuration (Fig 8).

FIGURE 9

A: Flat preparation of lower limbal palisades from a 23-year-old male illustrating standard palisade configuration. Individual papillae are highlighted by their lighter density which is in sharp contrast to heavy staining of epithelial cell population (hematoxylin and eosin, × 30). B: Thin, elongated palisades characteristic of superior limbus (hematoxylin and eosin, × 30).

HISTOLOGIC STUDIES

Flat Preparations

The overall topography of the palisades was revealed in these views. The lighter staining of the actual palisades was in sharp contrast to the almost overwhelming, densely stained cellular epithelial compartment. The stromal element within the palisade showed spindle-shaped fibroblasts embedded within loose subepithelial collagen and was delimited by pigment-bearing basal cells aligned in linear fashion. Figs 9 and 10A show

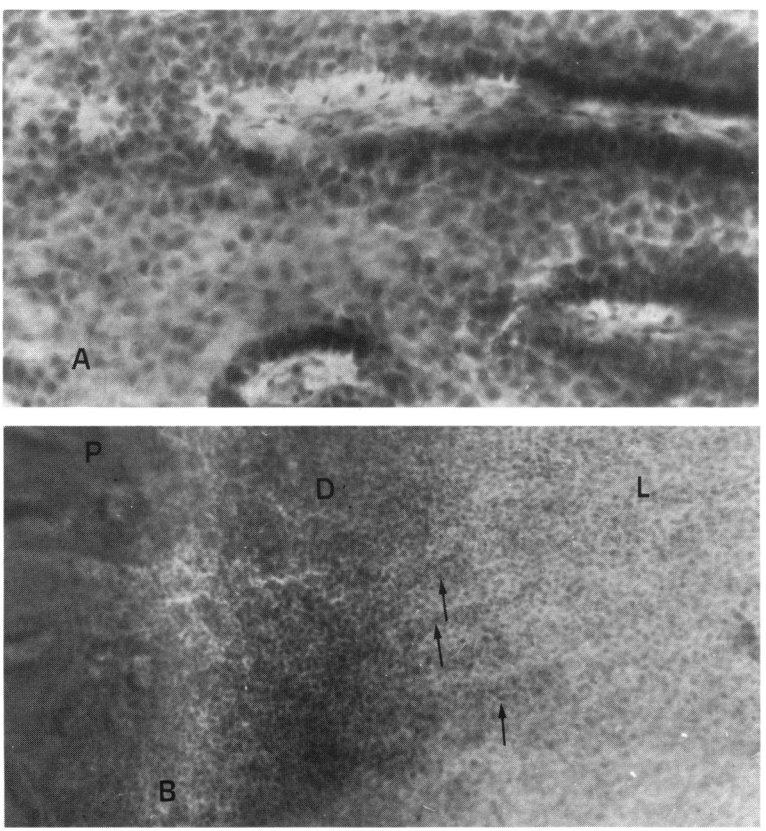

FIGURE 10

A: High-power view of flat preparation of horizontal quadrant from a 17-year-old male. Minuscule ovals and occasional cylindrical, short palisades were usually encountered in that region (hematoxylin and eosin, × 76). In this particular example, gross observation under dissecting microscope failed to reveal palisades. B: Flat preparation of lower limbal palisade region from a 34-year-old black female. Beyond the palisades themselves (P) a region of highest epithelial density (D) gives way to another, more central, lightly populated zone (L). Rows of pigmented basal cells in indian file cross from zone D to zone L in radial fashion (hematoxylin and eosin, × 30).

the palisade arrangement characteristic of each quadrant of the cornea. The rather stubby pattern of the lower limbal palisades gave way to the thin, elongated structures commonly seen superiorly. The horizontal pattern was that of scarce, minuscule ovals.

A gradient of epithelial cell density was apparent in the flat preparations. The epithelial cell population overlying the palisades region changed centrally to a denser zone; a third zone within the cornea again showed a decrease in cell density. In the area of transition between the latter two zones, it was possible to observe linear, radially oriented projections of pigment-bearing basal cells that crossed from one zone to the other (Fig 10B).

Serial Sections

Serial sections cut in the longitudinal plane parallel to the palisades presented a view along the length of the structure. The palisades were seen to begin some distance from Bowman's layer and peripheral to the capillaries within the conjunctival substantia propria (Fig 11A). The basement membrane of the corneal epithelium became irregular toward the end of Bowman's layer. Although the limbal epithelium showed slight thickening at this point, the palisade itself did not appear until the end of the limbal region. At that point, the number of basal cell nuclei increased abruptly, marking the site of the first rete ridge (Fig 11B).

Serial cross sections showed the prominent mounds of subepithelial papillae, the palisades themselves, as well as the broader rete ridges covering them (Fig 12A). The rete ridges appeared as projections of stratified epithelium of rectangular shape directed downward into the stroma and separated into blocks by the papillary elevations. The thin epithelial cell population covering the papillary crests consisted of four or five cell layers; the rete pegs included 15 layers of cells, which differed from the epithelial cells that covered the rest of the ocular surface. Unlike the conjunctival epithelium, the rete peg epithelium appeared devoid of goblet cells. Unlike the corneal epithelium, the rete peg basal cells appeared cuboidal rather than columnar and the nucleus showed no tendency to occupy an apical position. Furthermore, melanocytes were commonly seen dispersed among the basal cells of the rete pegs (Fig 12B), a finding not present in the cornea but one that explains the frequent presence of melanin granules within the basal cell cytoplasm.

The basal cell population lining the rete ridges appeared no different morphologically from the population covering the papillary crests (Fig 13). In this region, the overlying cells were arranged in three or four layers, in contrast to the nearly 15 layers of the rete ridge. The cells of the

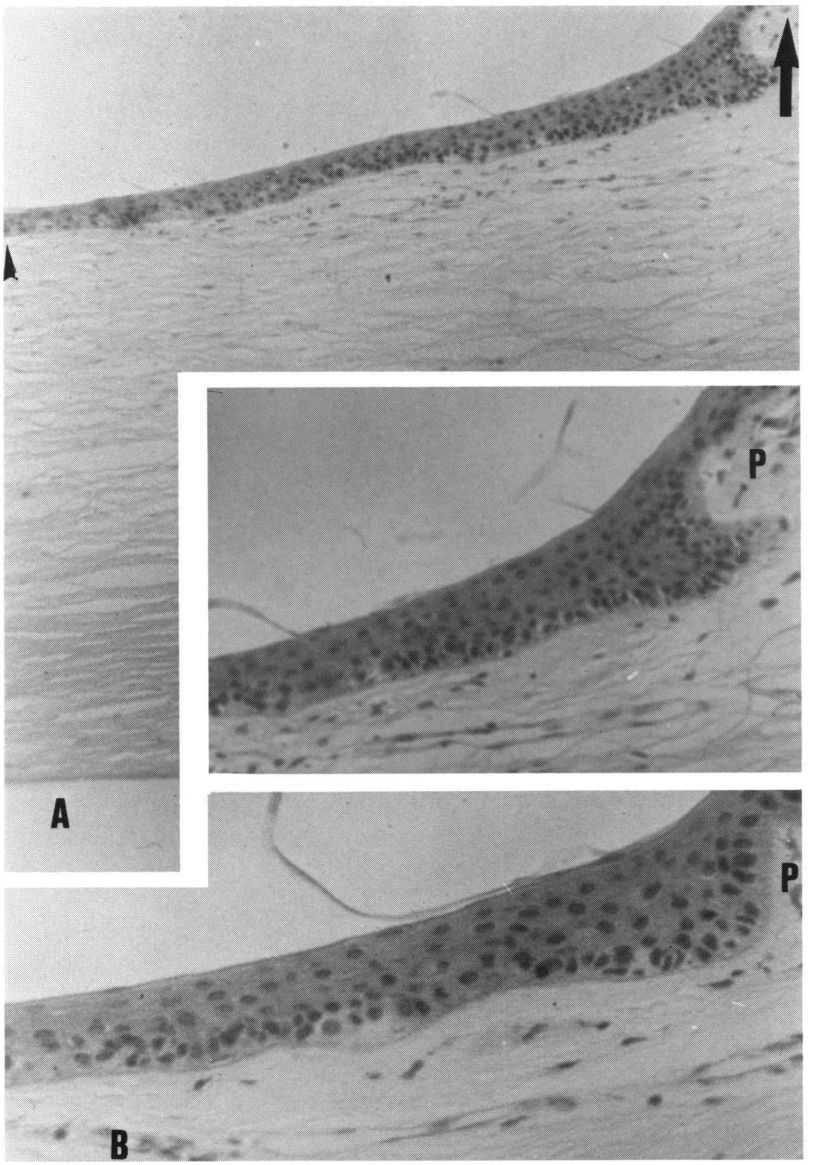

FIGURE 11

A: Longitudinal section of inferior limbus. Bowman's layer (*small arrow*) is separated from proximal end of palisades (*large arrow*) by whole width of limbus (hematoxylin and eosin, × 50). INSET: Higher power view of limbal epithelium. Basal cells are crowded together within actual palisades in either direction (hematoxylin and eosin, × 100). B: Higher power of same region from another subject showing decrease in nuclei away from palisade region (P) (hematoxylin and eosin, × 325).

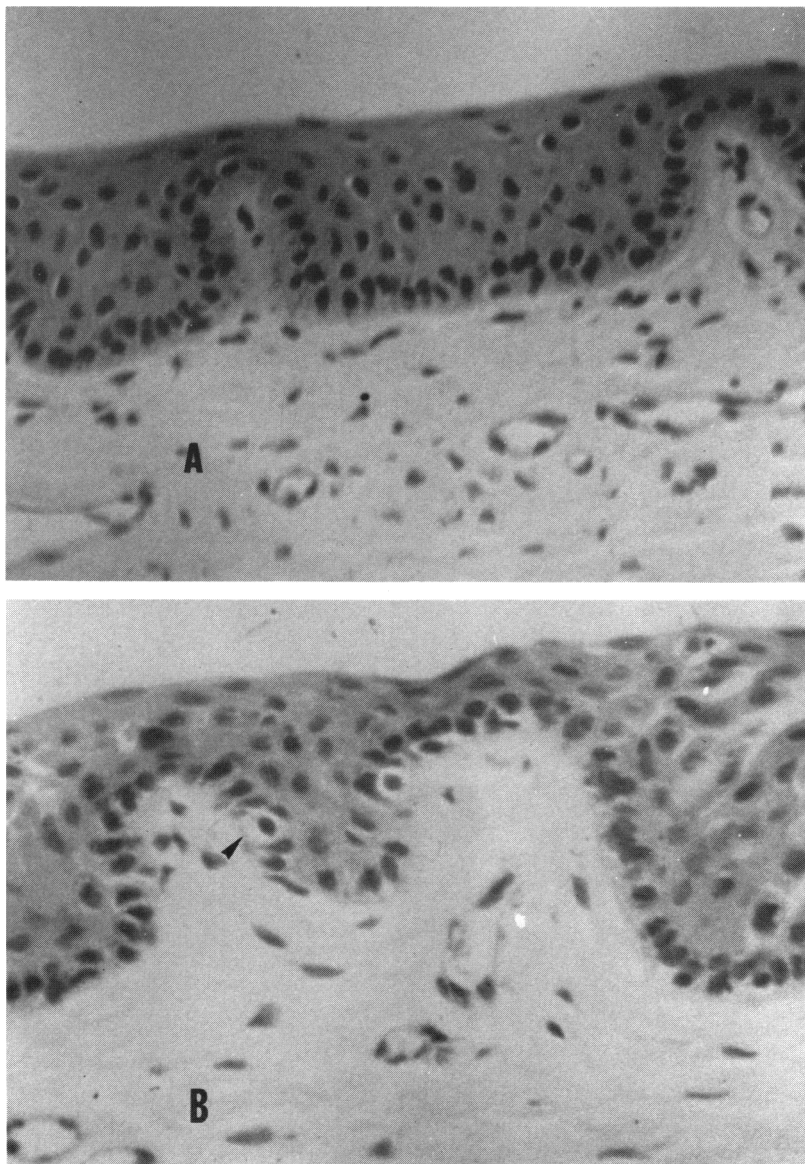

FIGURE 12
A: Cross section of palisades. Subepithelial papillae form triangular mounds that divide the rete ridges into rectangular projections directed downward toward stroma (hematoxylin and eosin, × 350). B: Cross section of inferior limbal palisades from another subject. No goblet cells are present but melanocytes are seen at basal cell level (*arrow*) (hematoxylin and eosin, × 375).

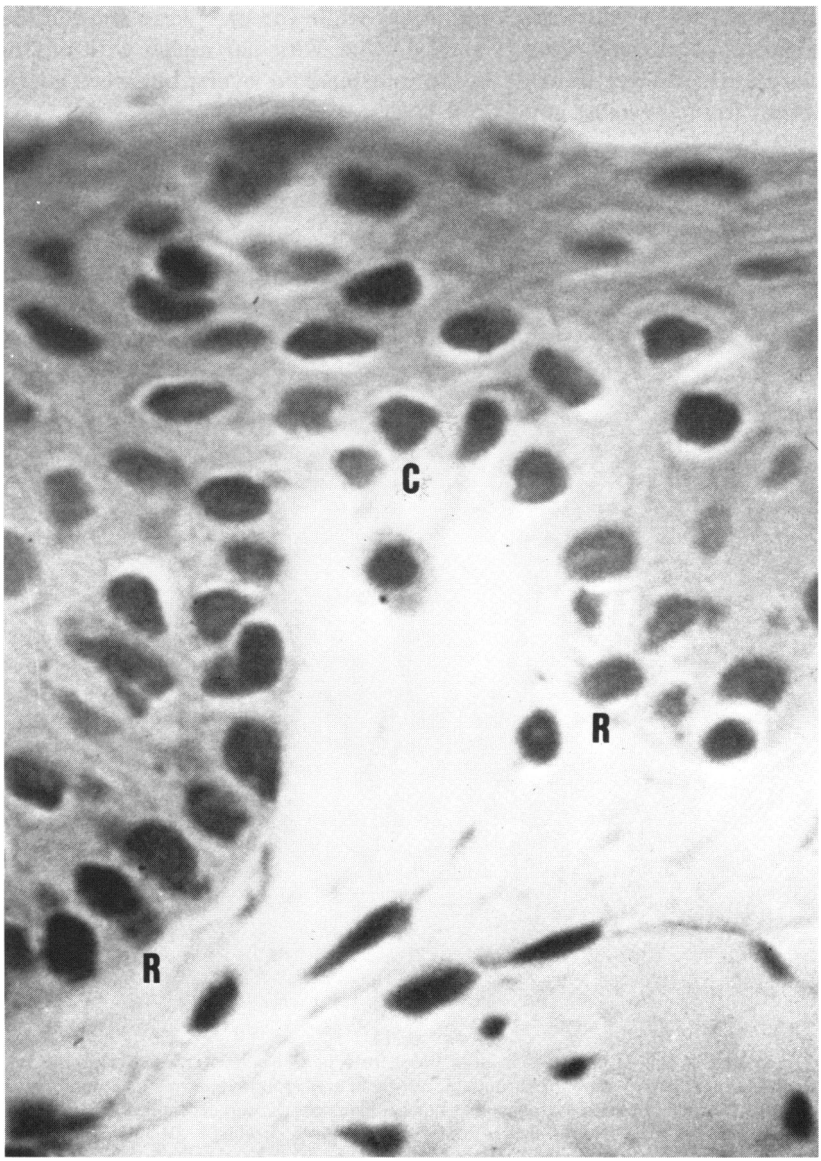

FIGURE 13
High-power view of inferior limbal palisades. Basal cell population of rete peg (R) shows no significant difference from that covering the apex of the papilla (C). In both populations, cells are cuboidal, with large, centered, dense nuclei (hematoxylin and eosin, × 825).

more superficial layers appeared larger while the cytoplasm showed the eosinophilia characteristic of keratohyalin. Vesicular nuclei with one or more nucleoli were the rule in the intermediate layers, but were totally absent from the most superficial layers.

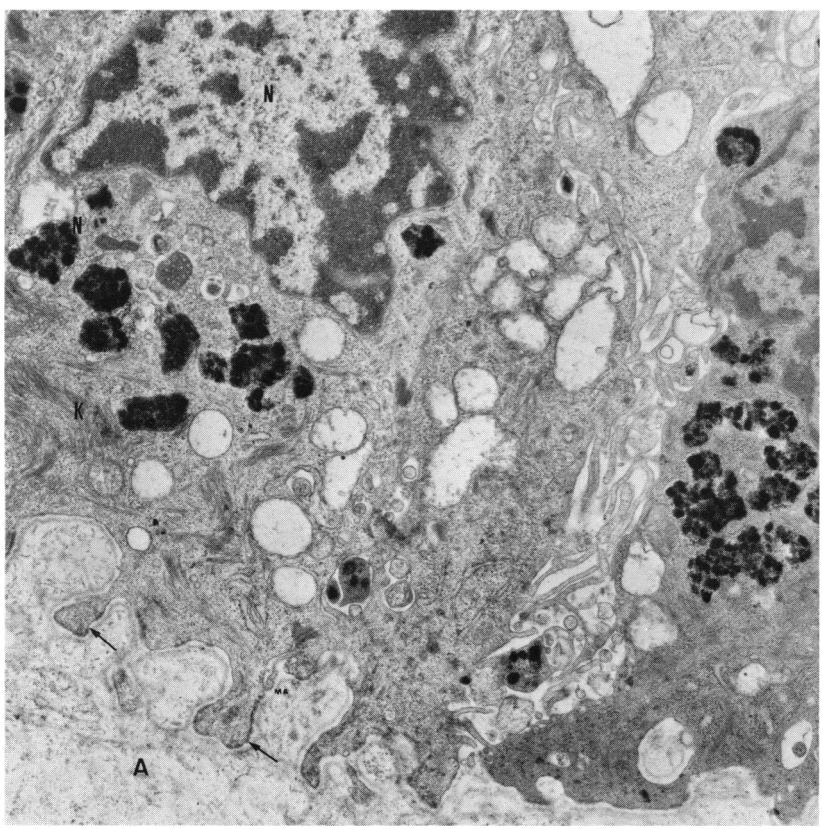

FIGURE 14

A: Typical basal cell of palisades in area lining rete peg. Nucleus (N) shows prominent indentations and clumped heterochromatin, mostly in area around inner nuclear membrane. Abundant melanin granules (N), as well as keratin filaments (K) and organelles are scattered within cytoplasm. Blunt-tipped ruffles (*arrows*) project into stroma (× 10,000). B: Solitary, small, round, electron-dense basal cell wedged between other basal cells. Scanty cytoplasm (*arrow*) shows few organelles (× 10,000).

ULTRASTRUCTURE

The rete pegs over the palisade region showed characteristic basal cells (Fig 14A) that were cuboidal in shape, with centrally located nuclei. The nuclei were relatively large, accounting for more than a third of the cell area; they were round in shape with deep, prominent indentations. Heterochromatin was arranged in clumps, usually near the inner nuclear membrane. Nucleoli were present. The cytoplasm contained abundant

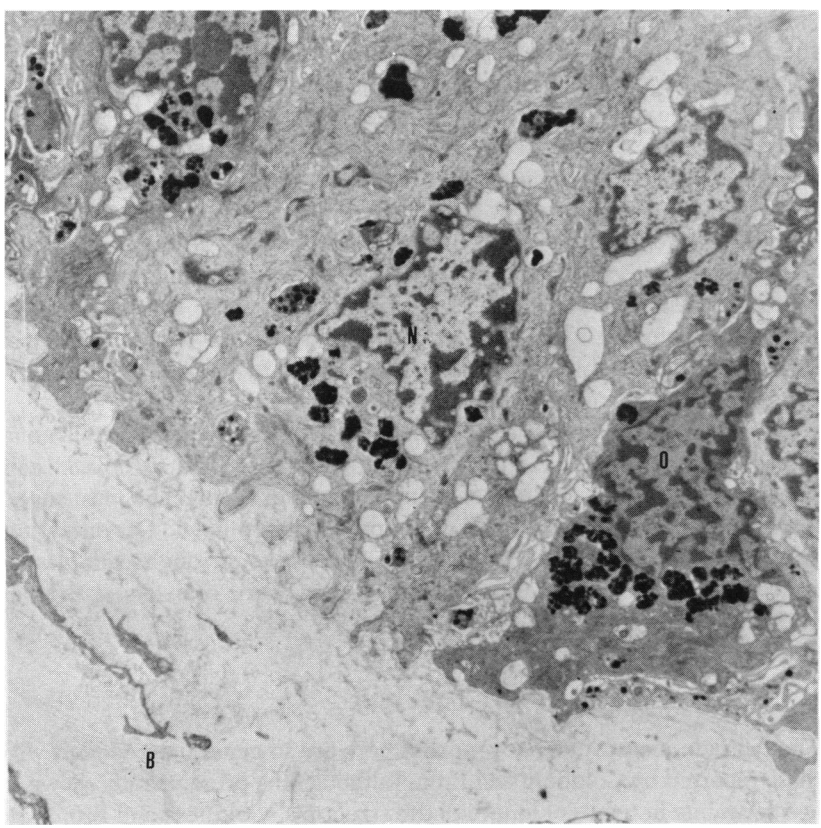

melanin granules, moderate amounts of keratin filaments, and a considerable number of organelles, including mitochondria, Golgi complexes, ribosomes, and rough endoplasmic reticulum. The intercellular spaces appeared wide. Prominent interdigitations and numerous desmosomes were seen. Along the undersurface, the cell membrane was thrown into numerous, short, blunt-tipped folds or ruffles directed toward the subepithelial tissue.

A second type of basal cell (Fig 14B), distinguishable by virtue of its smaller size and greater electron density, was seen scattered throughout the cell layer, wedged between the larger basal cells. These cells were considerably fewer in number and about half the size of the larger cells. The nuclei occupied most of the cell area; both the shape of the nuclei and the distribution of the chromatin were similar to what was seen in the larger basal cells. The scarce cytoplasm contained some melanin granules and vesicular structures, but few mitochondria or other organelles. The undersurface of the cell membrane appeared ruffled, although to a lesser degree than in the other type of basal cell. Intermediate forms between these two basal cells were observed frequently (Fig 15). The intermediate forms were similar to the small, dark basal cells in terms of electron density, but resembled the more common, larger basal cells in size, cytoplasmic area, and cytoplasmic organelles.

The cells occupying the intermediate layers displayed a polygonal shape and prominent vesicular, convoluted nuclei. The cytoplasm contained numerous keratin filaments and melanin granules. The most superficial cells showed a fusiform shape. Some lacked nuclei. Degenerating, poorly defined organelles, as well as a few stacks of rough endoplasmic reticulum, filled the cytoplasm. A few folds were seen along the cell surface.

DISCUSSION

The palisade measurements reported here are in general agreement with those reported by Goldberg and Bron,[8] although the present study showed a greater range in terms of length of the structure. Goldberg and Bron[8] also described frequent variations in the shape and morphology of the individual palisade, as was observed biomicroscopically in the present study.

It is possible to correlate palisade length with limbal width in a given individual. Compared with the palisades of the inferior limbus, which measured an average of 0.31 mm in length, the palisades of the superior limbus were longer and thinner, as if they had been stretched. This finding was readily apparent in the flat preparations (Fig 9B). Perhaps the

lengthening of the superior limbus that normally occurs during the early years of life carries the palisade along with it. In the well-developed anterior segment, the superior limbus is nearly double the size of the inferior limbus, and this relationship was frequently seen in the length of the palisades. In the horizontal quadrants, where the limbus is less than half the size of the lower limbus, the palisades were minuscule, when detectable at all (Fig 3B).

It would be difficult to postulate an important role for the palisade complex in the continuous renewal of the epithelium if this structure

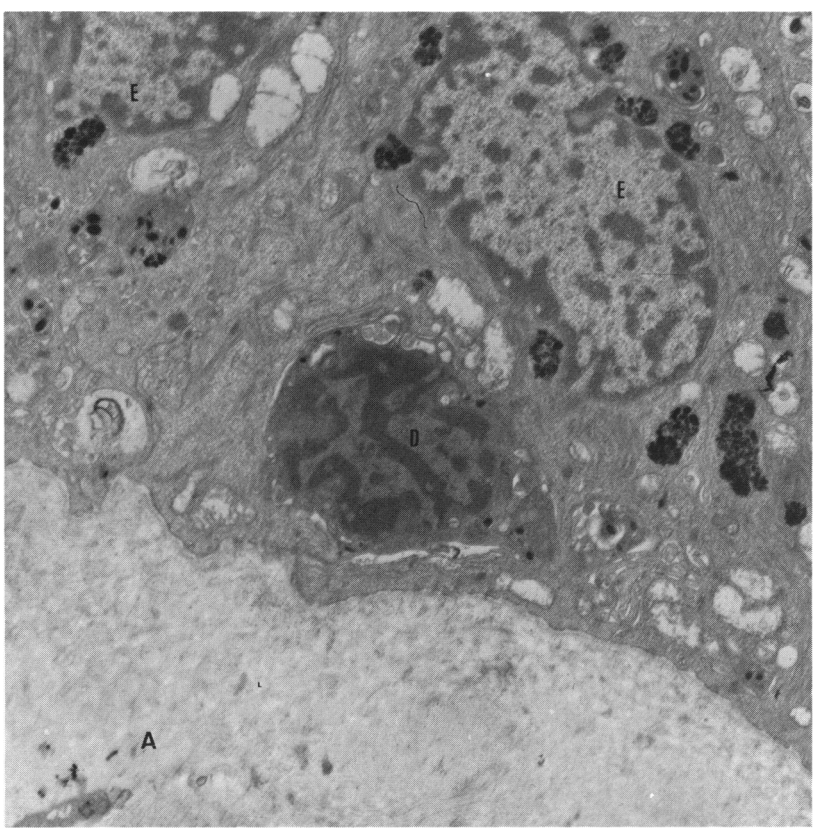

FIGURE 15

A: Dark basal cell (D) lies under two other basal cells (E) that are more electron dense than typical basal cells shown in Fig 14A. However, they share some similarities with the typical basal cell, such as size, cytoplasmic area, location of heterochromatin, and organelles (× 9000). B: Basal cell on left (N) shows typical pattern; basal cell on right (O) is more electron dense (× 9000).

were truly absent from as much as 20% of the normal population. However, the inability to detect a structure by biomicroscopy does not prove its absence. Indeed, miniature palisades were observed microscopically in flat preparations from limbal areas that appeared empty on gross examination with the dissecting microscope. When the horizontal and the vertical meridians were compared in the flat preparations, the relative scarcity of palisades in the horizontal meridians was revealed. Despite this, the overall epithelial cell density showed no dramatic difference between the two regions, a finding difficult to reconcile with the possible role of the palisade as the source of stem cells. There is no question, however, that the limbal region holds the greatest population density of basal epithelial cells, as demonstrated by the flat preparations (Fig 10B).

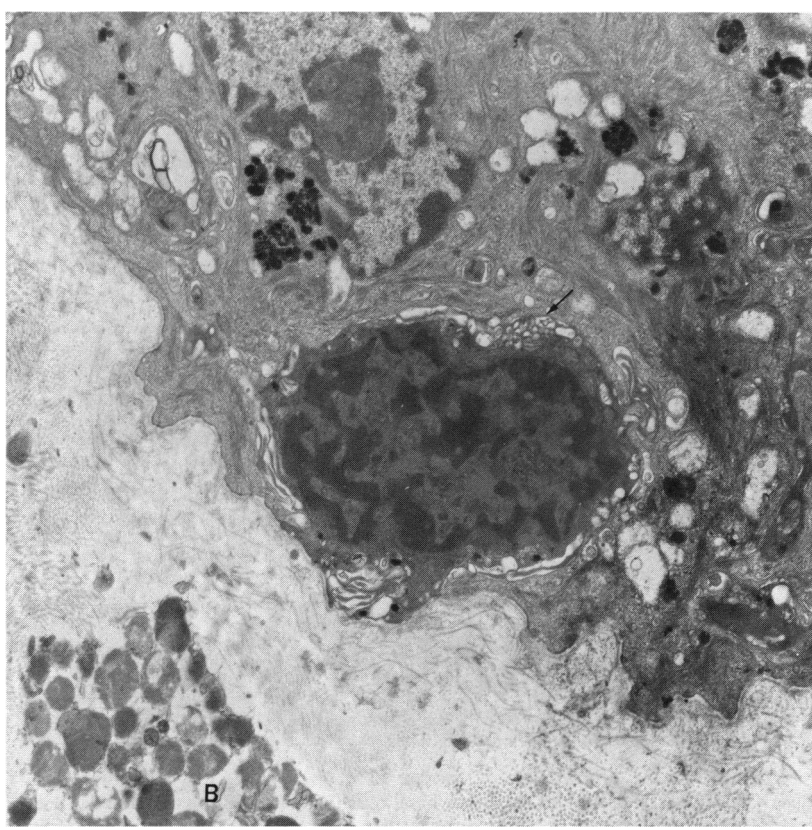

In addition, the infoldings that characterize the palisade region exceed those in every other region in the epibulbar surface. These infoldings must generate a considerably greater area, one bearing basal cells, than any other region on that surface.

Figure 11B illustrates the large number of basal cells that are crowded together in the palisade region, and the progressive reduction in density as the cells move toward the cornea or conjunctiva. Also, the more superficial layers, which are more numerous in this region, provide a greater population density of superficial cells than any other region. This cellular richness implicates this region as the site of the proliferative compartment, if an analogy can be made with other organ systems.

The radially disposed lines of basal cells streaming across the limbal zone revealed in the flat preparations (Fig 10B) are a striking finding in harmony with the ceoncept of centripetal transit in the undisturbed cornea. Pigmented individuals frequently bear yellow-brown streaks that are visible through the biomicroscope with high magnification and that may reflect a view of the basal cell horizontal transit (Fig 3A). Fluorescein applied topically to the cornea of patients with chronic epithelial deficits, as described above, disclosed the staining of linear streaks which were quite similar to the yellow-brown streaks noted in pigmented individuals. These streaks formed a vortex or spoke-wheel pattern when fully developed, as noted in the five case reports (Figs 4 to 8). Bron[36] described similar streaks in patients during the resurfacing of corneal abrasions and identified this same vortex pattern in many other conditions. All of these cases were characterized by the accumulation of cytoplasmic deposits, whether from endogenous or exogenous sources. He postulated that such deposits marked the cells, making visible their centripetal transit from the limbus across the corneal surface. Such a vortex pattern is also vividly illustrated, although unrecognized as such, in published descriptions of several other disorders, including Sieman's disease, Meldersson-Rosenthal syndrome, acrodermatitis enteropathica, and granular dystrophy.[73] The fully developed vortex, spoke-wheel, or verticillate patterns, all remarkably similar regardless of the clinical setting, may be viewed as tracing the lateral epithelial transit of the cornea (Fig 16A). Partial patterns may appear depending on the situation and locus of major deposition or epithelial stress (Fig 16B to E).

Any hypothetical model of horizontal epithelial transit must reconcile the known relatively rapid vertical turnover, as well as the greater mitotic rate of the peripheral cells, with the apparently very slow horizontal slide reported by Buck.[33] In the model shown in Fig 17A, the basal cell alternates between a horizontal mitosis and the slide of a new cell. Such a

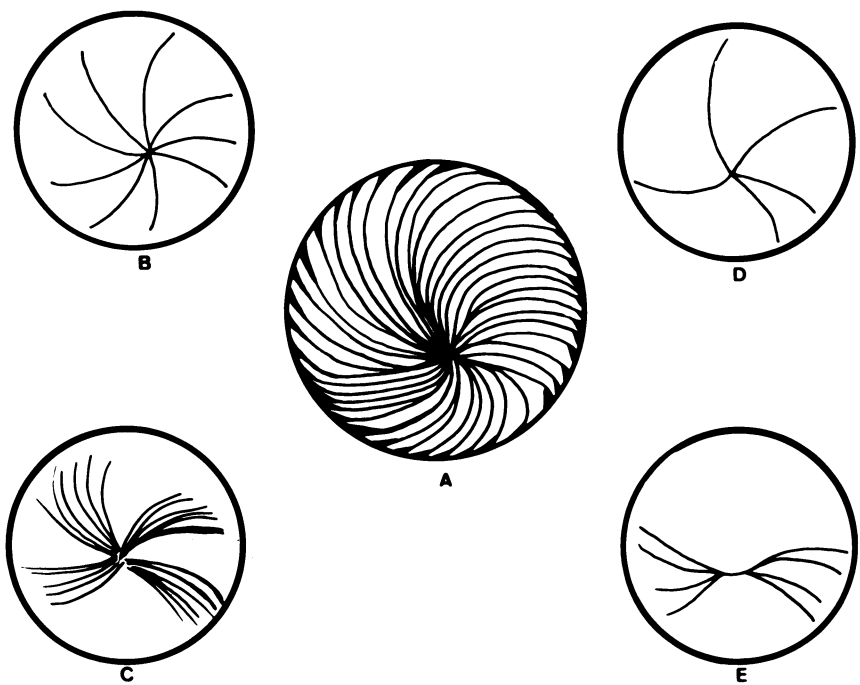

FIGURE 16
Vortex or spoke-wheel pattern that may present when horizontal epithelial transit is unveiled. A illustrates complete pattern; B through E show incomplete variants that tend to predominate under clinical conditions.

system would result in a very rapid lateral transit and similar mitotic rates across the cornea from periphery to center, features which are not consonant with the known facts. The model shown in 17B calls for two vertical mitoses before the new progenitor basal cell slides in from the periphery. Here mitotic rate is greater peripherally while the surface loss rate is

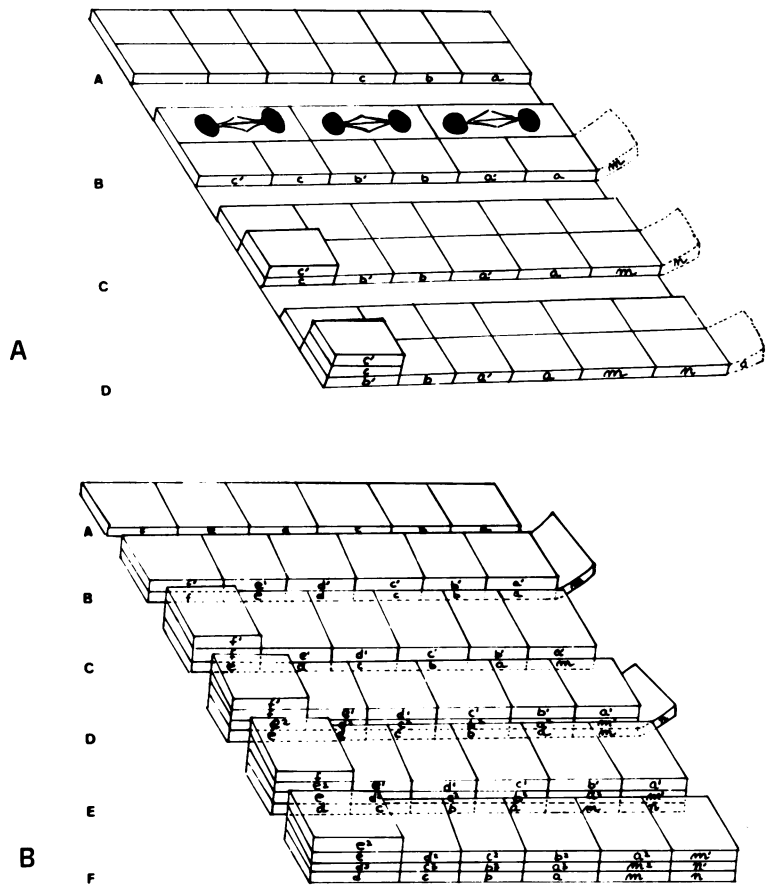

FIGURE 17

Hypothetical models of epithelial transit and turnover. Model shown in A uses horizontal mitoses alternating with slide of a new basal cell (m, n, o). Model shown in B is favored as being closer to real situation. Here, mitoses are vertical and two take place before new basal cell slides in from periphery.

greater centrally (an unknown factor). The presumed centripetal transit is much slower. This model is more in tune with the little that is known about the overall transit of the basal cell.

The basal cells of the palisades, at the ultrastructural level, revealed an interesting morphologic heterogeneity not appreciated by light microscopy. The characteristic and common basal cells (Fig 14A) were very different from the sparser, small, round, electron-dense cells (Fig 14B). (These electron-dense basal cells must not be confused with the "dark cells" of the old literature, which have been characterized by Perera[74] as fixation artifacts.) The typical basal cell showed features of differentiation such as organelles and a relatively large cytoplasmic area, in contrast to the smaller, electron-dense basal cell. The smaller cells may be considered to be relatively undifferentiated on the basis of their scarcity, small size, almost absent cytoplasm, and few organelles.[14] Morphologically "intermediate" forms that formed a spectrum between the two extremes of differentiation were seen; these cells could represent daughter cells on their way toward differentiation.

It may be that, within the system of cell renewal, the small, round, electron-dense basal cells are the actual stem cells of the corneal epithelium. Differentiating daughter basal cells, labeled as progenitor cells, mature with each division, yet remain basal cells within the lower level compartment. Eventually some migrate upward while others move centripetally in the horizontal plane. There were no ultrastructural differences between the basal cells lining the rete pegs and those over the papillary crests. Both showed blunt ruffling comparable to the nonserrated basal cells described in the epidermis.[25]

Most clinicians have witnessed the rapid re-epithelialization of the corneal surface which usually follows a superficial lamellar keratectomy. In many cases, the entire limbal epithelium, with the contained palisades, is removed. Evidently, the conjunctiva is capable of self-renewal, a property that has been amply confirmed in the literature.[75] This fact strongly suggests the existence of a generous supply of stem cells throughout the conjunctival surface.

CONCLUSIONS

The palisades of Vogt are limbal ridges averaging 0.31 mm in length and forming annular rows of approximately 36 individual units per limbal quadrant. Biomicroscopic observation of the palisades in 200 individuals assigned to six groups revealed a low prevalence (30%) for this standard pattern. The palisades showed a general tendency to be prominent in the

lower limbus, attenuated but lengthened superiorly, and undetectable in the horizontal quadrants.

Flat preparations confirmed the patterns observed biomicroscopically. In addition, areas that appeared grossly without palisades revealed the presence of these structures on microscopic examination. These preparations showed the palisade region to contain three zones of epithelial density; the most dense zone occupied a position adjacent to the palisades. Basal cells aligned in file crossed the cell population zones radially.

Longitudinal sections revealed that the basal cell concentration was greatest in the palisade region and waned with increasing proximity to either the cornea or the conjunctiva. The individual palisades appeared as papillae that were triangular in shape with the apex pointing upward. The palisade crests were covered by only a few layers of epithelial cells. Adjacent to the crests, prominent, thick, rectangular rete ridges extended downward into the subepithelial connective tissue.

By light microscopy the basal cell population of the palisades appeared cuboidal and homogeneous, save for the presence of scattered melanocytes. Electron microscopy, however, revealed a heterogeneous basal cell population composed of cells with varying degrees of differentiation. The most undifferentiated basal cells appeared as small, round, electron-dense cells with scanty cytoplasm. These morphologic features are similar to those of the stem cell population in other tissues.

The same linear streak pattern tracing the surface migration of pigment-bearing and deposit-filled epithelial cells was observed also with fluorescein application in patients with chronic epithelial disease. When fully developed, such streaks formed a vortex or spoke-wheel pattern. This pattern appears to represent the transit pathway for the differentiating basal cells as they move centripetally from the limbal palisades onto the cornea.

REFERENCES

1. Duke-Elder S, Wybar KC: The anatomy of the visual system, in S Duke-Elder (ed): *System of Ophthalmology*. St Louis, CV Mosby, 1961, p 112.
2. Dubreuil J: The human limbus. *Rev Gen Histol* 1906; 8:695-709.
3. Voft A: *Atlas of the Slitlamp-Microscopy of the Living Eye*. Berlin, Springer-Verlag, 1921, p 23.
4. Aurell G, Kornerup T: On glandular structures at the corneoscleral junction in man and swine: The so-called "Manz glands." *Acta Ophthalmol* 1949; 27:19-40.
5. Duke-Elder S, Wybar KC: The anatomy of the visual system, in S Duke-Elder (ed): *System of Ophthalmology*. St Louis, CV Mosby, 1961, p 115.
6. Davanager M, Evensen A: Role of the pericorneal papillary structure in renewal of corneal epithelium. *Nature* 1971; 229:560-561.
7. Lemp MA: Cornea and sclera: Annual review. *Arch Ophthalmol* 1976; 94:473-490.

8. Goldberg MF, Bron AJ: Limbal palisades of Vogt. *Trans Am Ophthalmol Soc* 1982; 80:155-171.
9. Smolin G, Thoft RA: *The Cornea: Scientific Foundations and Clinical Practice*. Boston, Little, Brown, 1983.
10. Brightbill FS: *Corneal Surgery: Theory, Technique, and Tissue*. St Louis, CV Mosby, 1986.
11. Hanna C, O'Brien JE: Cell production and migration in the epithelial layer of the cornea. *Arch Ophthalmol* 1960; 64:536-539.
12. Hanna C, O'Brien JE: Cell turnover in the adult human eye. *Arch Ophthalmol* 1961; 65:695-698.
13. Leblond CP: The life history of cells in renewing systems. *Am J Anat* 1981; 169:114-155.
14. Cairnie AB, Lala PK, Osmond DG (eds): *The Stem Cells*. New York, Academic Press, 1976.
15. Cairnie AB, Lamerton LF, Steel GG: Cell proliferation studies in the intestinal epithelium of the rat: II. Theoretical aspects. *Exp Cell Res* 1965; 39:539-555.
16. Cormack DH: *Ham's Histology*. Philadelphia, JB Lippincott, 1987, p 47.
17. Baserga R: The cell cycle. *N Engl J Med* 1981; 304:453-459.
18. Allen TD, Potten CS: Fine-structural identification and organization of the epidermal proliferative unit. *J Cell Sci* 1974; 15:291-319.
19. Potten CS, Allen TD: The fine structure and cell kinetics of mouse epidermis after wounding. *J Cell Sci* 1975; 17:413-447.
20. Pinkus H, Meheregan AH: *A Guide to Dermatohistopathology*. St Louis, CV Mosby, 1982, p 13.
21. Bertalanffy FD, Lau C: Cell renewal. *Int Rev Cytol* 1962; 78:357-365.
22. Mackenzie IC, Fusenig NE: Regeneration of organized epithelial structure. *J Invest Dermatol* 1983; 81:189s-194s.
23. Schermer A, Galvin S, Sun TT: Differentiation-related expression of a major 64K corneal keratin in vivo and in culture suggests limbal location of corneal epithelial stem cells. *J Cell Biol* 1986; 103:49-56.
24. Lavker RM, Sun TT: Heterogeneity in epidermal basal keratinocytes: Morphological and functional correlation. *Science* 1982; 215:1239-1241.
25. ———: Epidermal stem cells. *J Invest Dermatol* 1983; 81:121s-126s.
26. Buschke W, Friedenwald JS, Fleischman W: Studies on the mitotic activity of the corneal epithelium. *Bull J Hopkins Hosp* 1943; 73:143-150.
27. Maumenee AE: Repair in the cornea, in W Mongtagna, RE Billingham (eds): *Advances in Biology of Skin*. New York, Macmillan Co, 1964, vol 5.
28. Ebato B, Friend R, Thoft RA: Comparison of central and peripheral human corneal epithelium in human culture. *Invest Ophthalmol Vis Sci* 1987; 28:1450-1456.
29. Kaye DB: Epithelial response in penetrating keratoplasty. *Am J Ophthalmol* 1980; 89:381-387.
30. Kinoshita S, Friend J, Thoft RA: Sex chromatin in donor corneal epithelium in rabbits. *Invest Ophthalmol Vis Sci* 1981; 21:434-440.
31. Shapiro MS, Friend J, Thoft RA: Corneal re-epithelialization from the conjunctiva. *Invest Ophthalmol Vis Sci* 1981; 21:134-142.
32. Buck RC: Cell migration in repair of mouse corneal epithelium. *Invest Ophthalmol Vis Sci* 1979; 18:767-784.
33. ———: Centripetal migration in mouse corneal epithelium. *Invest Ophthalmol Vis Sci* 1985; 26:1296-1300.
34. Mann I: A study of epithelial regeneration in the living eye. *Br J Ophthalmol* 1944; 28:26-40.
35. Cowan T: Striate melanokeratosis in Negroes. *Trans Am Ophthalmol Soc* 1963; 61:61-74.
36. Bron AJ: Vortex patterns of the corneal epithelium. *Trans Ophthalmol Soc UK* 1973; 93:455-471.

37. Thoft RA, Friend J: The X, Y, Z hypothesis of corneal epithelial maintenance. *Invest Ophthalmol Vis Sci* 1983; 24:1442-1443.
38. Arey LB, Covode WM: Method of repair in epithelial wounds of cornea. *Anat Rec* 1943; 86:75-86.
39. Friedenwald JS, Buschke W: Mitotic and wound-healing activities of the corneal epithelium. *Arch Ophthalmol* 1944; 32:410-413.
40. Bullough WS: The chalones. *Science* 1969; 5:71-73.
41. Friedenwald JS, Buschke W: Some factors concerned in the mitotic and wound healing activities of the corneal epithelium. *Trans Am Ophthalmol Soc* 1944; 42:371-383.
42. McDonald J, Wilder H: The effect of beta radiation on corneal healing. *Am J Ophthalmol* 1953; 40:170-179.
43. Borgers M, Debrabander M (eds): *Microtubules and Microtubule Inhibitors*. Amsterdam, North Holland, 1975.
44. Elliott JH, Leibowitz HM: The influence of immunosuppressive agents upon corneal wound healing. *Arch Ophthalmol* 1966; 76:334-337.
45. Gundersen T, Liebman SD: Effect of local anesthetics on regeneration of corneal epithelium. *Arch Ophthalmol* 1944; 31:29-35.
46. Beuerman RW, Schimmelpfennig B: Sensory denervation of the rabbit cornea affects epithelial properties. *Exp Neurol* 1980; 69:196-201.
47. Sigelman S, Friedenwald JS: Mitotic and wound-healing activities of corneal epithelium: Effect of sensory denervation. *Arch Ophthalmol* 1954; 52:46-57.
48. Butterfield LC, Neufeld AH: Cyclic nucleotides and mitosis in the rabbit cornea following superior cervical ganglionectomy. *Exp Eye Res* 1977; 25:427-433.
49. Smelser GK: The influence of vehicles and form of penicillin and sulfonamides on mitosis and healing of corneal burns. *Am J Ophthalmol* 1946; 29:541-543.
50. Friedenwald JS, Buschke W: The effects of excitement, of epinephrine and of sympathectomy on the mitotic activity of the corneal epithelium in rats. *Am J Physiol* 1944; 141:689-694.
51. Burns ER, Roberson M, Shock JP, et al: Circadian rhythmicity, cell kinetics, and flow cytometry of corneal epithelium. Presented at the 1987 Meeting of the Association for Research in Vision and Ophthalmology, Sarasota, Florida, May 1987. *Invest Ophthalmol Vis Sci* (Suppl) 1987; 28:7.
52. Friedenwald JS, Buschke W, Morris ME: Mitotic activity and wound healing in corneal epithelium of vitamin A-deficient rat. *J Nutr* 1945; 29:299-310.
53. Hunt TE: The effect of nutrition on mitotic activity. *Anat Rec* 1957; 127:539-550.
54. Sigelman RN, Dohlman C, Friedenwald JS: Effects of hypophysectomy. *Arch Ophthalmol* 1954; 52:751-754.
55. Friedenwald JS, Buschke W: Influence of some experimental variables on epithelial movements in healing of corneal wounds. *J Cell Comp Physiol* 1944; 23:95-107.
56. Mauger TF, Hill RM: Corneal epithelial healing in hypoxic environments. Presented at the 1987 Meeting of the Association for Research in Vision and Ophthalmology, Sarasota, Florida, 1987. *Invest Ophthalmol Vis Sci* (Suppl) 1987; 28:2.
57. Kuwabara T, Perkins DG, Cogan DG: Sliding of the epithelium in experimental corneal wounds. *Invest Ophthalmol Vis Sci* 1976; 15:4-14.
58. Marr WG, Wood R, Seuterfit L, et al: Effect of topical anesthetics on regeneration of corneal epithelium. *Am J Ophthalmol* 1957; 43:606-610.
59. Srinivasan BD, Kulkarni PS: The effect of steroidal and non-steroidal anti-inflammatory agents on corneal re-epithelialization. *Invest Ophthalmol Vis Sci* 1981; 20:688-691.
60. Nishida T, Nakagawa S, Awata T, et al: Fibronectin promotes epithelial migration of cultured rabbit cornea in situ. *J Cell Biol* 1983; 97:1653-1656.
61. Buschke W, Friedenwald JS, Moses RA: Effect of ultraviolet radiation. *J Cell Comp Physiol* 1945; 26:147-152.
62. Foster CS, Pavan-Langston D: Corneal wound healing and antiviral medication. *Arch Ophthalmol* 1977; 95:2062-2067.

63. Bergmanson JR, Ruben ME, Chu TS: Effects of contact lenses. *Cornea* 1984; 3:109-113.
64. Pfister RR, Burstein N: The effects of ophthalmic drugs, vehicles and preservatives on corneal epithelium: A scanning electron microscope study. *Invest Ophthalmol Vis Sci* 1976; 15:246-259.
65. Smelser GK, Ozanics V: Effect of excision of lacrimal gland. *Am J Ophthalmol* 1953; 36:1545-1549.
66. Levenson S: Effect of desiccation on the corneal surface. *Ann Ophthalmol* 1973; 5:865-869.
67. Abdel-Khalek LMR, Williamson J, Lee WR: Morphological changes in the human conjunctival epithelium: II. In keratoconjunctivitis sicca. *Br J Ophthalmol* 1978; 45:223-227.
68. Gilbard JP, Carter JB, Sang DN, et al: Morphologic effects of hyperosmolarity on rabbit corneal epithelium. *Ophthalmology* 1984; 91:1205-1212.
69. Mackie IA: Corneal nerves and destructive disease of the cornea. *Trans Ophthalmol Soc UK* 1978; 98:343-348.
70. Pfister RR: The alkali burned cornea: I. Epithelial and stromal repair. *Exp Eye Res* 1976; 23:519-526.
71. Kanai A, Polack FM: Ultramicroscopic alterations of corneal epithelium in corneal grafts. *Am J Ophthalmol* 1971; 72:119-126.
72. Sheenan DZ, Hrapchak BB: *Histotechnology*. St Louis, CV Mosby, 1980.
73. Grayson M: *Diseases of the Cornea*. St Louis, CV Mosby, 1979, pp 445-452.
74. Perera RN: Basal cells of the corneal epithelium. *Br J Ophthalmol* 1969; 53:595-605.
75. Thoft RA: Biochemical transformation of regenerating ocular surface epithelium. *Invest Ophthalmol Vis Sci* 1977; 16:14-20.